


# Control for gravity compensation in tendon-driven upper limb exosuits

**Conference Paper****Author(s):**

Georgarakis, Anna-Maria; Song, Jaeyong; [Wolf, Peter](#) ; Riener, Robert; Xiloyannis, Michele

**Publication date:**

2020

**Permanent link:**

<https://doi.org/10.3929/ethz-b-000449812>

**Rights / license:**

[In Copyright - Non-Commercial Use Permitted](#)

**Originally published in:**

<https://doi.org/10.1109/biorob49111.2020.9224460>

# Control for gravity compensation in tendon-driven upper limb exosuits

Anna-Maria Georgarakis<sup>1,2</sup>, Jaeyong Song<sup>1</sup>, Peter Wolf<sup>1</sup>, Robert Riener<sup>1,2</sup> and Michele Xiloyannis<sup>1,2</sup>

**Abstract**—Soft wearable robots, or exosuits, are a promising technology to assist the upper limb during daily life activities. So far, several exosuit concepts have been proposed, some of which were successfully tested in open-loop control. However, though simple and robust, open-loop control is cumbersome and unintuitive for use in daily life. Here, we closed the control loop on the human-robot interface of the Myoshirt. The Myoshirt is an upper limb exosuit that supports the shoulder joint during functional arm elevation. A direct force controller (DF) as well as an indirect force controller (IF) were implemented on the Myoshirt to assess their suitability for autonomously tracking human movement. In a preceding testbench analysis, a direct force controller with linear friction compensation (DFF) could be excluded, as linearly compensating friction aggravated the force tracking error in the ramp response (RMSE mean|sd : 32.75|10.95 N) in comparison to the DF controller ramp response (27.61|9.38 N). In the same analysis, the IF controller showed substantially better tracking performance (17.12|0.99 N). In the subsequent movement tracking analysis including five participants (one female), the position tracking error and smoothness (median(RMSE), median(SPARC)) were similar with the DF (3.9°, -4.3) and IF (3.4°, -4.1) controllers and in an unpowered condition (3.7°, -4.2). However, the force tracking error and smoothness were substantially better when the IF controller (3.4 N, -4.5) was active than with the DF controller (10.4 N, -6.6). The magnitude response in the Bode analysis indicated that both controllers were obstructing the human movement at higher frequencies, however with 0.78 Hz, the IF controller satisfied the bandwidth requirement for daily life assistance, while the DF controller (0.63 Hz) did not. It can be concluded that the IF controller is most suitable for assisting human movement in daily life with the Myoshirt.

## I. INTRODUCTION

Impairments of the upper limbs can result in a substantial loss of quality of life as activities of daily living become tremendously harder to execute. The cause of an upper limb impairment may originate from various disorders, such as stroke or muscular dystrophies, but also from typical aging. For some of these disorders, the impairment may be irreversible, or even aggravate with time. Since the patients cannot be supported continuously by therapists, they generally learn to adapt to their limitations.

One proposed solution to assist the upper limb in daily life is based on the concept of soft, textile-based exoskeletons, so called exosuits. Exosuits serve the purpose of restoring the

range of motion and endurance of the upper limb, in particular the shoulder joint, of patients with moderate impairments. Until now, the designs of exosuits supporting the shoulder were primarily drawn upon biomechanical considerations [1]. Some of these approaches were successfully tested on healthy users and patients, showing a reduction in muscle activity when the device was active [2], [3]. However, these results were obtained with an open-loop control, where the device assistance was activated by pressing a button. While simple and robust, open-loop control is counter-intuitive and cumbersome for daily use.

To enable the exosuit to move with the user autonomously, the control loop must be closed at the human-robot interface. The closed-loop controller ought to accurately track a reference force with a high bandwidth to preserve the exosuit's mechanical transparency during movement. The compliant nature of the human-robot interface, as well as non-linear effects such as inertia and friction in the transmission system, can lead to unwanted interaction forces, which further raises the demands on the controller performance. Several control schemes are able to satisfy these requirements, which can be categorized as direct or indirect force controllers [4].

Direct force controllers have shown good performance in cable-driven systems, though they require additional model sophistication to compensate the non-linearities in the transmission system [5]. More recently, an indirect force controller was implemented in a study on an exosuit for gravity compensation of the elbow joint [6]. The proposed position-based indirect force controller, including an outer force and inner velocity feedback loop, appears promising for transfer to a gravity-assisting exosuit for the shoulder joint.

To date, there is a lack of evidence on the comparative performance of closed-loop controllers in tendon-driven exosuits. To address this gap, three different control schemes for supporting the shoulder joint against gravity were implemented. While the first two controllers directly control the assistive force, either with or without friction compensation, the third controller indirectly controls the assistive force by regulating the motor velocity.

The control schemes were implemented and evaluated on a tendon-driven exosuit for the upper limb, the Myoshirt. The Myoshirt was designed to support the shoulder against gravity during reaching in daily living tasks. Prior to an evaluation with human participants, the controllers' performance was elaborated on a testbench. The goal of both evaluation stages was to assess the force tracking accuracy and bandwidth of each control scheme when assisting human movement with the Myoshirt.

This work was supported by the Swiss National Center of Competence in Research (NCCR) Robotics

<sup>1</sup>A.-M. Georgarakis, J. Song, P. Wolf, R. Riener and M. Xiloyannis are with the Sensory-Motor Systems (SMS) Lab, Institute of Robotics and Intelligent Systems (IRIS), ETH Zurich, Switzerland [marie.georgarakis@hest.ethz.ch](mailto:marie.georgarakis@hest.ethz.ch)

<sup>2</sup>A.-M. Georgarakis, R. Riener and M. Xiloyannis are with the Reharobotics Group, Spinal Cord Injury Center, Balgrist University Hospital, Medical Faculty, University of Zurich, Switzerland

## II. METHODS

### A. Controller requirements

Arm elevation angles during activities of daily living approximately range from  $20^\circ$  to  $120^\circ$  with an average of  $68^\circ$  [7], [8]. Assuming that typical arm movements follow a minimum jerk trajectory [9] with a maximum average velocity of  $91.2^\circ s^{-1}$  [10], the peak velocity of arm elevation can be estimated to be  $171^\circ s^{-1}$ . Hence, for reaching the average height of  $68^\circ$  with an average velocity of  $91.2^\circ s^{-1}$ , the minimum required movement bandwidth can be determined to be  $\omega = 0.67$  Hz [8], [10].

Using anthropometry, the minimum required torque in the shoulder to be able to fully assist the 95<sup>th</sup> percentile of the male US-American population (weight 128.8 kg, height 1.87 m) is  $\tau_a = 20$  Nm [11], [12].

### B. Hardware

Our target movement was a coupled elevation and external rotation of the shoulder in the frontal plane, resulting in a one-dimensional movement trajectory. The trajectory was defined based on a large range of daily living activities [1] and implemented in the design of the Myoshirt, a tendon-based exosuit supporting the shoulder during daily living activities.

The Myoshirt comprised a thorax harness with a shoulder anchor point above the acromion and an arm cuff system with an anchor point on the upper arm, about 5 cm above the Medial Epicondyle of the elbow. The Myoshirt was actuated by a tendon that was routed between the two anchor points.

A motor (EC-i 40, Maxon Motor, Switzerland) wound up the tendon and thus applied an gravity-assistive force  $F_{ga}$ . Between the motor and the acromion anchor point, the tendon passed through a Bowden cable with a teflon liner. On the lower level, the motor was controlled by a motor controller (ESCON 50/5, Maxon Motor, Switzerland) running at 53.6 kHz for current and 5.36 kHz for speed control. On the higher level, the sensor data acquisition and controllers were implemented on a real-time operating system (FreeRTOS on FRDM-K66F, NXP Semiconductors, The Netherlands) running at 1 kHz.

Arm elevation was determined from the orientation of the gravitational vector within the reference frame of an Inertial Measurement Unit (IMU) (FSM300, Hillcrest Laboratories, MD, USA), which was mounted on the upper arm and sampled at 0.4 kHz. The assistive force was measured in proximity to the arm anchor with a load cell (LSB200 445 N, Futek, CA, USA, amplifier: A100, Futek, CA, USA) sampled at 1 kHz.

### C. Gravity-Assistance (GA) estimator

An exosuit applies an gravity-assistive force  $F_{ga}$  to generate a torque  $\tau_{ga}$  about a given joint. For the Myoshirt, this joint is the gleno-humeral joint (GH joint) in the shoulder. Here, the GH joint was simplified as a ball-and-socket joint. As the movement was performed in a plane, a two-dimensional approximation was performed to model the applied torques, see Figure 1.

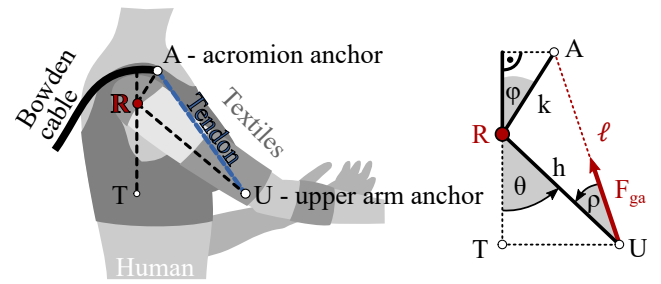


Fig. 1. Geometric considerations for the Gravity-Assistance estimator model. The arm elevation is defined as the angle  $\theta$  between the upper arm anchor point  $U$  and the torso reference point  $T$  around the center of rotation  $R$  of the gleno-humeral joint. The exosuit applies an assistive force  $F_{ga}$  through the tendon of length  $\ell$  (passing behind the arm) between the upper arm anchor point  $U$  and the acromion anchor point  $A$ .

The design of the Myoshirt was defined by the distances between the anchor points and the given anatomical landmarks. In the model, the fixed distance between the center of rotation of the GH joint  $R$  and the upper arm anchor  $U$  is denoted by  $h$ . The fixed distance between  $R$  and the anchor point on the acromion  $A$  is denoted by  $k$ . The distance between the anchor points  $A$  and  $U$ , which is the effective tendon length, is denoted by  $\ell$ .

The maximum torque acting on the shoulder due to gravity  $\tau_g$  can be obtained from geometric considerations and anthropometric data

$$\tau_g = m_{arm} \cdot g \cdot \ell_{arm} \sin(\theta), \quad (1)$$

with  $m_{arm}$  being the total mass of the user's arm,  $g$  being the gravity constant,  $\ell_{arm}$  being the distance of center of gravity of the extended arm from the center of rotation in the GH joint, and  $\theta$  being the arm elevation angle, assuming that  $h$  is roughly parallel to the principal arm axis. Both  $m_{arm}$  and  $\ell_{arm}$  are estimated using anthropometry and information about the user's body height and weight [11].

With a human wearing the exosuit,  $\tau_g$  can be compensated by the biological torque  $\tau_b$  contributed by the human, supplemented with the gravity-assistive torque  $\tau_{ga}$ .

$$\tau_g = \tau_{ga} + \tau_b \quad (2)$$

The gravity-assistive torque  $\tau_{ga}$  is generated by the assistive force  $F_{ga}$  in dependency on their orthogonal projection:

$$\tau_{ga} = F_{ga} \cdot h \cdot \sin(\rho) \quad (3)$$

with

$$\rho = \cos^{-1}\left(\frac{\ell^2 - k^2 + h^2}{2\ell h}\right). \quad (4)$$

Geometrically, the tendon length  $\ell$  is given by

$$\ell^2 = k^2 + h^2 - 2kh \cdot \cos(\pi - \theta - \varphi). \quad (5)$$

Hence, the required assistive force  $F_{ga}$  can be determined with

$$F_{ga} = \frac{\tau_g - \tau_b}{h \cdot \sqrt{1 - \left(\frac{h^2 + \ell^2 - k^2}{2\ell h}\right)^2}}. \quad (6)$$

For the 95<sup>th</sup> percentile of the male US-American population, this complies with a maximum assistive force of  $F_{ga} = 259.5$  N at  $\theta = 90^\circ$  shoulder elevation.

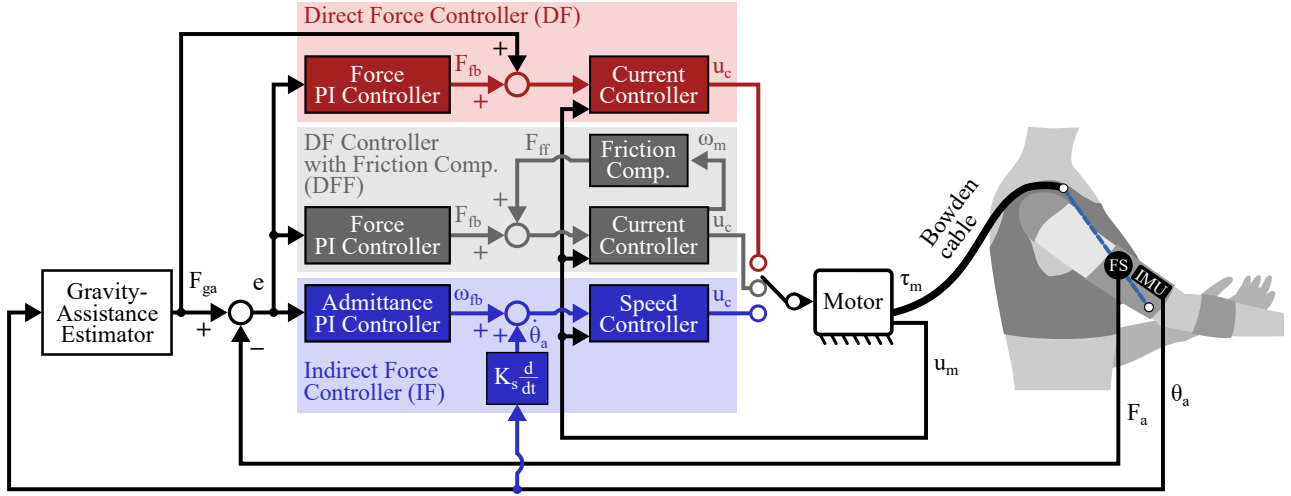


Fig. 2. Control schemes. The Gravity-Assistance (GA) estimator provides the reference force  $F_{ga}$  based on the current arm elevation  $\theta_a$ , measured by the IMU on the upper arm cuff. Three controllers were implemented on the exosuit actuation system, all of which take the error  $e$  between the reference force  $F_{ga}$  and the current assistive force  $F_a$ , that is measured by the load cell LC, as input. The DF controller directly controls the force error  $e$ , while the DFF controller additionally compensates for friction based on the current motor velocity  $\omega_m$ . Both control schemes provide a force feedback  $F_{fb}$  and regulate the motor current on the motor controller level. In contrast, the IF control scheme engages an admittance controller that provides a motor velocity feedback  $\omega_{fb}$  and regulates the motor velocity  $\omega_m$  on the motor controller level. An additional feed-forward term based on the arm elevation velocity  $\dot{\theta}_a$  increases the adaptation speed of the IF controller.

#### D. Control Schemes

Three closed-loop control schemes were implemented on the Myoshirt, see Figure 2. Each control scheme was designed such that it would track a fraction of  $\tau_g$ , thus supporting the user's movement against gravity. The estimated gravity-assistive force  $F_{ga}$  therefore served as reference, and the measured human-robot interaction  $F_a$  as force feedback. Thus, for all controllers, the control input  $e(t)$  is defined as

$$e(t) = F_{ga} - F_a. \quad (7)$$

The general form of the PI controllers implemented in each control scheme is

$$u_{fb} = P_i e(t) + I_i \int_0^t e(t) dt \quad (8)$$

where  $u_{fb}$  is the feedback of the PI controller, and  $P_i$  and  $I_i$  are the proportional and integral gains, respectively.

1) *DF — Closed-loop direct force controller with gravity-assistance feed-forward:* The DF controller regulates the assistive force  $F_a$  at the upper arm anchor point to the estimated GA reference force  $F_{ga}$ , which serves as the feed-forward set point.

$$F_{DF} = F_{fb} + F_{ga} \quad (9)$$

where the controller feedback  $u_{fb} = F_{fb}$  is given by (8) with  $P_i = P_{DF}$  and  $I_i = I_{DF}$ .

2) *DFF — Closed-loop direct force controller with friction compensation:* To improve the reactivity of the actuation, a second control scheme based on the DF controller, but with feed-forward friction compensation  $F_{ff}(\omega_m)$ , was implemented. Here,  $F_{ff}(\omega_m)$  models both static and viscous friction and the controller feedback.

$$F_{DFF} = F_{fb} + F_{ff}(\omega_m) \quad (10)$$

where the controller feedback  $u_{fb} = F_{fb}$  is given by (8) with  $P_i = P_{DFF}$  and  $I_i = I_{DFF}$ .

To identify the model for static and viscous friction, the actuation system including the Bowden cable was attached to a fixed frame. A weight of 0.5 kg was suspended from the tendon to identify the point of stiction as well as viscous friction. Both static and viscous friction, depending on the motor velocity  $\omega_m$ , were compensated according to

$$F_{ff}(\omega_m) = \begin{cases} 20 \text{ N} & , \text{ if } \omega_m \leq 0.59 \text{ s}^{-1} \\ 0.93 \text{ N s} \cdot \omega_m + 10.6 \text{ N} & , \text{ otherwise.} \end{cases} \quad (11)$$

3) *IF — Closed-loop indirect force controller:* Other than the direct force controllers, that regulate the torque  $\tau_m$  on the motor level, the indirect force controller regulates the angular velocity  $\omega_m$  [4], [13]. To generate the required reference velocity, the interaction torque feedback  $\tau_a$  is regulated to the GA reference  $\tau_{ga}$  by an admittance controller with the transfer function

$$H(s) = \frac{\omega_{fb}}{\tau_{ga} - \tau_a} = K_P + K_I s^{-1}, \quad (12)$$

with gains  $K_P$  and  $K_I$  in the Laplace domain. Using (3),

$$\tau_{ga} - \tau_a = c \sin(\rho) e(t), \quad (13)$$

and thus the controller feedback term  $u_{fb} = \omega_{fb}$  can be written in the time domain with (8), where  $P_i = P_{IF}$  and  $I_i = I_{IF}$ . Moreover, a positive feedback term, proportional by the gain  $K_s$  to the user's movement velocity  $\dot{\theta}_a$ , is added to the controller [14]. The positive feedback term improves the reactivity of the controller, and therefore increases its bandwidth. Consequently, the desired motor velocity  $\omega_{IF}$  can be determined with

$$\omega_{IF} = \omega_{fb} + K_s \dot{\theta}_a. \quad (14)$$

### E. Testbench analysis — Force tracking

For the initial evaluation of the controllers, the anchor points were fixed on a rigid frame. Both the step and ramp response were assessed for each controller for forces up to 150 N, equivalent to a 50% support of the maximum assistive force, to evaluate their rise time, settling time and overshoot. For the step response, a square wave profile with  $\omega_{ref} = 0.125$  Hz frequency, 50% duty cycle and increasing force amplitudes was used as reference.

$$F_{ref}^{step}(t) = (\text{sgn}(\sin(2\pi \cdot \omega_{ref} \cdot t)) + 1) \cdot \lceil \frac{t}{8s} \rceil \cdot 7.5 \text{ N} \quad (15)$$

For the ramp response, a ramp function was used.

$$F_{ref}^{ramp}(t) = \begin{cases} \max(t, 0) \cdot 50 \text{ N s}^{-1} & \text{if } t < 3 \text{ s} \\ 150 \text{ N} & \text{if } 3 \text{ s} \leq t \leq 6 \text{ s} \\ 0 \text{ N} & \text{if } t > 6 \text{ s} \end{cases} \quad (16)$$

To pre-evaluate the force bandwidth, a sinusoid reference with increasing frequency was used, ranging from  $\omega_{ref} = 0.05$  Hz to 2.5 Hz.

$$F_{ref}^{sin}(t) = (1 + \sin(2\pi\omega_{ref}t)) \cdot 75 \text{ N} \quad (17)$$

### F. Functional controller analysis — Movement tracking

Based on the results of the testbench analysis, the DFF controller was excluded from the subsequent functional analysis. To expose the remaining controllers to different dynamic human-robot behaviors, five participants (one female, age [22...25] years, weight [53...80] kg, height [1.60...1.90] m) were included. Two additionally recruited participants had to be excluded due to fitting issues. The measurements were approved by the ethics commission of ETH Zurich in accordance with the Declaration of Helsinki (EK 2019-N-165). All participants were volunteers and gave written informed consent to participate in the analysis.

Each controller was tested once with each participant in randomized order. For each controller, assistance was set to support 70% of  $\tau_g$ . Additionally, participants performed the experiments without assistance, but wearing the cuff and sensor systems. After a familiarization period, participants were instructed to elevate and lower their arms following a position reference trajectory on a screen. Participants received visual feedback of their current position. As position reference, a sinusoidal trajectory was used to approximate the minimum jerk trajectory in Section II-A.

$$\theta_{ref} = 50^\circ + 40^\circ \sin(2\pi\omega_{ref}t) \quad (18)$$

The tested frequencies ranged from  $\omega_{ref} = 0.1$  Hz to 1 Hz, see Figure 4. Each frequency lasted for a minimum of five periods.

### G. Data analysis

All data was sampled with 200 Hz directly from the microcontroller. Before analysis, the angle and force data was low-pass filtered at 10 Hz through a  $2^{nd}$ -order Butterworth filter. Velocity data was derived by differentiating angle data.

TABLE I  
TESTBENCH ANALYSIS  
(mean | standard deviation)

	Step response			Ramp response	
	overshoot (in %)	rise time (in s)	settling time (in s)	RMSE (in N)	St.Dev. (in N)
DF	—	0.63   0.79	1.59   1.19	27.61	9.38
DFF	—	0.71   0.35	1.44   1.41	32.75	10.95
IF	18.6   7.5	<b>0.27</b>   <b>0.02</b>	<b>0.68</b>   <b>0.34</b>	<b>17.12</b>	<b>0.99</b>

The tracking accuracy was analyzed by means of the root mean square error (RMSE) between reference  $\bullet_{ref}$  and measured quantity  $\bullet_a$

$$RMSE = \sqrt{\frac{1}{n} \sum_{t=t_0}^T (\bullet_{ref} - \bullet_a)^2}. \quad (19)$$

To analyze the frequency response, a Bode analysis was performed. To define the force bandwidth, the half-power point definition was used, i.e. the input frequency for which the magnitude of the system response drops below  $-3$  dB.

The tracking ability of the controllers in terms of movement smoothness was analyzed using the spectral arc length (SPARC) between reference and measured force [15].

## III. RESULTS

### A. Testbench measurements — Force tracking

The results of the step and ramp responses are summarized in detail in Table I and Figure 3. For the sinusoidal input, only the indirect force controller could be analyzed for its cut-off frequency, which was determined to be 2.35 Hz. The dynamics of both direct force controllers were not suitable for identifying the cut-off frequency in the Bode diagram as the magnitude did not satisfy the  $-3$  dB criterion for the lowest tested frequencies.

### B. Functional controller analysis — Movement tracking

All participants were able to complete the measurement protocol. The results of the movement tracking in position and force during the functional controller analysis are summarized in Figure 5. From the results of the sinusoidal tracking analysis, a Bode diagram was created. Due to the human response, the human-robot-interaction forces increased with the frequency. Therefore, the  $-3$  dB criterion was inverted to determine the cut-off frequency. The cut-off frequency of the DF controller was identified to be 0.63 Hz, for the IF controller the cut-off frequency was 0.78 Hz, see Figure 4.

## IV. DISCUSSION

### A. IF controller showed best tracking performance.

The indirect force (IF) controller, comprising of an inner velocity and an outer force feedback loop, outperformed the direct force (DF and DFF) controllers. The performance supremacy of the IF controller was reflected in a lower force tracking error and a higher movement smoothness, see Table I and Figure 5, and higher bandwidth, see Figure 4, both in the testbench analysis and during the functional analysis with human participants.

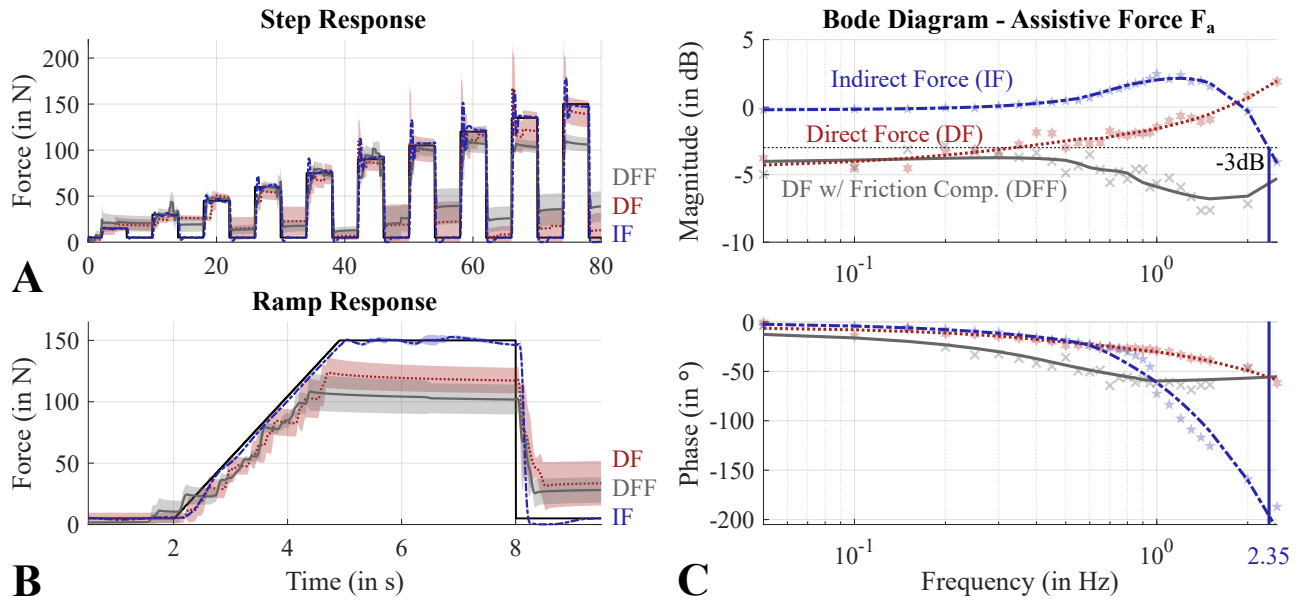


Fig. 3. Force tracking performance of the Myoshirt actuation system for three different control schemes. For this evaluation, the Myoshirt tendon was tethered to a fixed point on a rigid frame. (A) Step response with increasing force amplitudes. The force level was switched every four seconds. (B) Ramp response. The force level was increased to 150 N over 3 s. (C) For the Bode analysis, the reference force represented a sinusoidal trajectory with increasing frequencies and a constant amplitude of 150 N.

The main reason for the IF performance supremacy is the ability of the high-gain inner velocity feedback loop, closed at the motor level, to compensate for unwanted dynamics in the transmission system. This type of indirect force control, or “collocated admittance control” [4], allows to bypass the need for complex backlash- and friction-compensating models [16].

#### B. DF and DFF controllers unable to cope with stiction.

Indeed, despite calibrating the friction model carefully, the system response observed in Figure 3(A) and 3(B) indicate

that neither the DF nor the DFF controller were able to cope with the stiction effect. This phenomenon was particularly severe for slower changes in the force reference when the DF controller was engaged, see Figure 3(B). At higher frequencies, and hence with increasing force gradients, the direct force controller tended to overshoot, resulting in a raise of the magnitude of the system response in the Bode analysis, see Figure 3(C).

The friction model that was added in the DFF controller compensated for these overshoots when tested in a fixed configuration on the testbench, however, the applied steady-state force at the end effector was diminished. As the friction is non-linearly depending on the state of the transmission system, e.g. the Bowden cable curvature, it is extremely hard to model universally. The deficits in the DFF model accuracy could be compensated by tuning the controllers with higher and therefore stiffer gains. This, however, would come at the cost of the system’s stability. As a consequence, the DFF controller was excluded from the subsequent analysis.

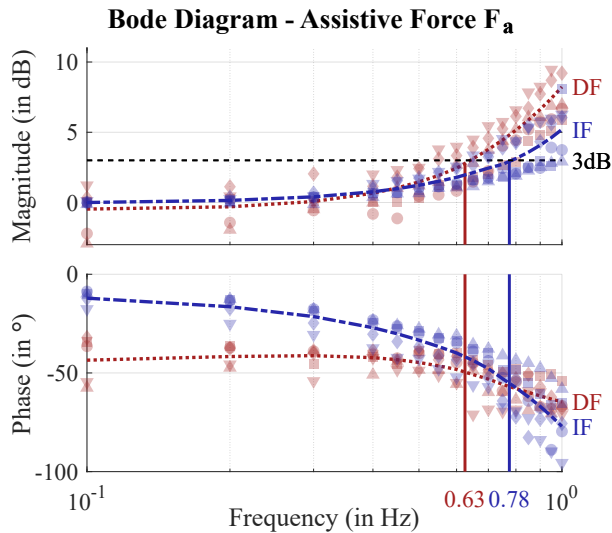


Fig. 4. Bode diagram for the controller evaluation on the Myoshirt with five participants, represented by markers. For both controllers, the assistive force  $F_a$  increases with increasing movement frequency due to the human-robot interaction. Therefore, the threshold of +3 dB was used to determine the cut-off frequencies, which were 0.68 Hz for the DF controller, and 0.82 Hz for the IF controller.

#### C. Powered exosuit does not obstruct position tracking.

For all participants, position tracking accuracy did not differ for powered and unpowered conditions, see Figure 5. This suggests that the controllers were transparent enough to allow for movement frequencies up to 1 Hz.

#### D. Interaction forces increased with movement frequency.

For movements at frequencies higher than the cut-off frequencies, the interaction forces between the user and the Myoshirt increased substantially, see Figure 4. The higher magnitude and phase shift of the force transfer function at higher frequencies suggest that the controller behavior obstructed the movement, particularly at the turn-over points.



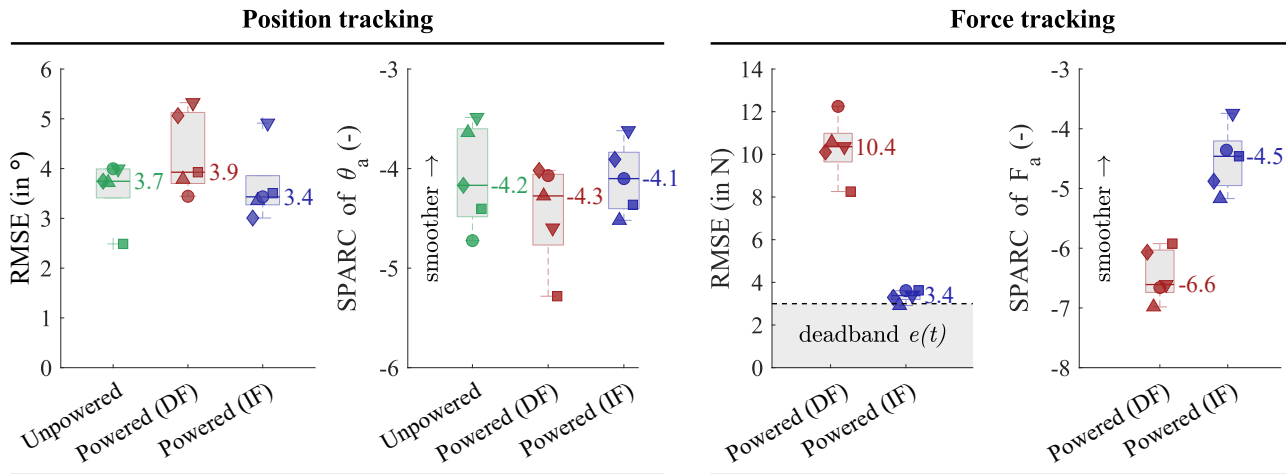


Fig. 5. Movement tracking performance during the minimum jerk trajectory evaluation. Horizontal lines and values represent medians, boxes represent 25<sup>th</sup> and 75<sup>th</sup> percentiles, symbols represent the five participants. With the controllers engaged, the tracking error (RMSE) and movement smoothness (SPARC) in arm elevation  $\theta_a$  were in the same range as in the unpowered condition. For the indirect force (IF) controller, the RMSE in force was close to the deadband of  $e(t) = 3$  N, within which the controller was deactivated. Due to the higher human-robot interaction forces, the RMSE in force was much higher for the direct force (DF) controller. The same tendency was visible when looking at the force tracking smoothness, where the IF controller allowed for smoother movements than the DF controller.

The cut-off frequency of the IF controller satisfied the bandwidth requirement. This was not true for the DF controller. The IF controller, moreover, demonstrated less phase shift for the lower frequencies, indicating a smaller delay between the reference and the performed movement.

### E. Limitations

This study focused on the relative performance of the investigated controllers rather than trying to optimize their absolute performance. For example, the baseline performance of both direct and indirect controllers could be improved by implementing a compliance model of the exosuit (following [13]), or by revising other hardware properties [5].

In addition, the force and position metrics employed in this analysis provide only indirect evidence of the provided assistance. Further insights could be obtained by investigating muscle activation patterns through electromyography.

## V. CONCLUSIONS

Implementing an indirect force controller, comprising of an outer force and inner high-gain velocity loop, is the more suitable and pragmatic approach than implementing a direct force controller for providing gravity assistance in a tendon-driven upper limb exosuit.

## REFERENCES

- [1] A.-M. Georgharakis, P. Wolf, and R. Riener, "Simplifying exosuits: Kinematic couplings in the upper extremity during daily living tasks," in *2019 IEEE 16th International Conference on Rehabilitation Robotics (ICORR)*. IEEE, 2019, pp. 423–428.
- [2] N. Li, T. Yang, P. Yu, J. Chang, L. Zhao, X. Zhao, I. H. Elhadj, N. Xi, and L. Liu, "Bio-inspired upper limb soft exoskeleton to reduce stroke-induced complications," *Bioinspiration & Biomimetics*, vol. 13, no. 6, p. 66001, 2018. [Online]. Available: <http://stacks.iop.org/1748-3190/13/i=6/a=66001>
- [3] C. T. O'Neill, N. S. Phipps, L. Cappello, S. Paganoni, and C. J. Walsh, "A soft wearable robot for the shoulder: Design, characterization, and preliminary testing," *IEEE International Conference on Rehabilitation Robotics*, vol. 02129, pp. 1672–1678, 2017.
- [4] A. Calanca, R. Muradore, and P. Fiorini, "A review of algorithms for compliant control of stiff and fixed-compliance robots," *IEEE/ASME Transactions on Mechatronics*, vol. 21, no. 2, pp. 613–624, 2015.
- [5] A. Schiele, P. Letier, R. Van Der Linde, and F. Van Der Helm, "Bowden cable actuator for force-feedback exoskeletons," in *2006 IEEE/RSJ International Conference on Intelligent Robots and Systems*. IEEE, 2006, pp. 3599–3604.
- [6] M. Xiloyannis, D. Chiaradia, A. Frisoli, and L. Masia, "Physiological and kinematic effects of a soft exosuit on arm movements," *Journal of neuroengineering and rehabilitation*, vol. 16, no. 1, p. 29, 2019.
- [7] D. J. Magermans, E. K. J. Chadwick, H. E. J. Veeger, and F. C. T. Van Der Helm, "Requirements for upper extremity motions during activities of daily living," *Clinical Biomechanics*, vol. 20, no. 6, pp. 591–599, 2005.
- [8] J. Aizawa, T. Masuda, T. Koyama, K. Nakamaru, K. Isozaki, A. Okawa, and S. Morita, "Three-dimensional motion of the upper extremity joints during various activities of daily living," *Journal of Biomechanics*, vol. 43, no. 15, pp. 2915–2922, 2010.
- [9] T. Flash and N. Hogan, "The coordination of arm movements: an experimentally confirmed mathematical model," *Journal of neuroscience*, vol. 5, no. 7, pp. 1688–1703, 1985.
- [10] F. Fayad, G. Hoffmann, S. Hanne-ton, C. Yazbeck, M.-M. Lefevre-Colau, S. Poiraudau, M. Revel, and A. Roby-Brami, "3-d scapular kinematics during arm elevation: effect of motion velocity," *Clinical biomechanics*, vol. 21, no. 9, pp. 932–941, 2006.
- [11] P. De Leva, "Adjustments to zatsiorsky-seluyanov's segment inertia parameters," *Journal of biomechanics*, vol. 29, no. 9, pp. 1223–1230, 1996.
- [12] National Center for Health Statistics (NCHS), "National Health and Nutrition Examination Survey (NHANES) 2015-16," Department of Health and Human Services, Centers for Disease Control and Prevention, Hyattsville, MD, U.S., 2016.
- [13] G. Lee, Y. Ding, I. G. Bujanda, N. Karavas, Y. M. Zhou, and C. J. Walsh, "Improved assistive profile tracking of soft exosuits for walking and jogging with off-board actuation," in *2017 IEEE/RSJ International Conference on Intelligent Robots and Systems (IROS)*. IEEE, 2017, pp. 1699–1706.
- [14] H. Kazerooni, J.-L. Racine, L. Huang, and R. Steger, "On the control of the berkeley lower extremity exoskeleton (bleex)," in *Proceedings of the 2005 IEEE international conference on robotics and automation*. IEEE, 2005, pp. 4353–4360.
- [15] S. Balasubramanian, A. Melendez-Calderon, A. Roby-Brami, and E. Burdet, "On the analysis of movement smoothness," *Journal of neuroengineering and rehabilitation*, vol. 12, no. 1, p. 112, 2015.
- [16] B. K. Dinh, M. Xiloyannis, C. W. Antuvan, L. Cappello, and L. Masia, "Hierarchical cascade controller for assistance modulation in a soft wearable arm exoskeleton," *IEEE Robotics and Automation Letters*, vol. 2, no. 3, pp. 1786–1793, 2017.